PNAS RESEARCH ARTICLE | BIOCHEMISTRY

Fibroblast growth factor 8b (FGF-8b) enhances myogenesis and inhibits adipogenesis in rotator cuff muscle cell populations in vitro

Takayoshi Otsuka[a,b], Ho-Man Kan[a,b], Paulos Y. Mengsteab[a,b,c,d], Breajah Tyson[a], and Cato T. Laurencin[a,b,c,d,e,f,1]

Contributed by Cato T. Laurencin; received August 23, 2023; accepted November 24, 2023; reviewed by Guillermo Ameer and Justin Hanes

Fatty expansion is one of the features of muscle degeneration due to muscle injuries, and its presence interferes with muscle regeneration. Specifically, poor clinical outcomes have been linked to fatty expansion in rotator cuff tears and repairs. Our group recently found that fibroblast growth factor 8b (FGF-8b) inhibits adipogenic differentiation and promotes myofiber formation of mesenchymal stem cells in vitro. This led us to hypothesize that FGF-8b could similarly control the fate of muscle-specific cell populations derived from rotator cuff muscle involved in muscle repair following rotator cuff injury. In this study, we isolate fibro-adipogenic progenitor cells (FAPs) and satellite stem cells (SCs) from rat rotator cuff muscle tissue and analyzed the effects of FGF-8b supplementation. Utilizing a cell plating protocol, we successfully isolate FAPs-rich fibroblasts (FIBs) and SCs-rich muscle progenitor cells (MPCs). Subsequently, we demonstrate that FIB adipogenic differentiation can be inhibited by FGF-8b, while MPC myogenic differentiation can be enhanced by FGF-8b. We further demonstrate that phosphorylated ERK due to FGF-8b leads to the inhibition of adipogenesis in FIBs and SCs maintenance and myofiber formation in MPCs. Together, these findings demonstrate the powerful potential of FGF-8b for rotator cuff repair by altering the fate of muscle undergoing degeneration.

fibroblast growth factor 8b | rotator cuff | fibro-adipogenic progenitor cells | satellite stem cells | muscle degeneration

Significance

Muscle degeneration, including fatty infiltration, muscle atrophy, and fibrosis, is associated with higher rotator cuff repair retear rates. In the present study, we isolate fibro-adipogenic progenitor cells (FAPs) and satellite stem cells (SCs) from rat rotator cuff muscle tissue and analyzed the effects of fibroblast growth factor 8b (FGF-8b) supplementation. We demonstrate that myogenic differentiation can be enhanced by FGF-8b, while adipogenic differentiation can be inhibited by FGF-8b. We further demonstrate that phosphorylated ERK is involved in the fate control of these cell populations. These results suggest the potential of FGF-8b application for rotator cuff repair by enhancing resident cell regeneration capability.

Chronic rotator cuff tears often lead to muscle degeneration which includes fatty expansion of the muscle as well as muscle atrophy and fibrosis (1–4). Studies have elucidated that fibro-adipogenic progenitor cells (FAPs) have been the source of fatty expansion during muscle degeneration in recent years (5–7). Furthermore, clinical studies have shown that higher retear rates of rotator cuff repair are associated with a more significant presence of fat, indicating that fatty expansion can be a prognostic marker of rotator cuff repair outcomes (8). Therefore, studying interventions modulating the amount of fat derived from FAPs may be a powerful potential therapeutic method to enhance muscle and tendon regeneration. Several biological factors are currently being explored for their therapeutic potential of rotator cuff repair, including various growth factors, stem cells, and stem cell–derived exosomes (9–13).

A previous study focusing on the effects of fibroblast growth factor 8b (FGF-8b) on controlling the fate of mesenchymal stem cells found that FGF-8b could both inhibit adipogenesis and promote myogenesis (14). By supplementing FGF-8b to differentiation mediums, such as myogenic and adipogenic mediums, we were able to identify the gain or loss of function due to this growth factor. However, it was not known whether the effects of FGF-8b would translate to muscle-specific cell populations, such as satellite stem cells (SCs) or FAPs, which play critical roles in pathologic and regenerative muscle processes.

FAPs are a heterogeneous population of cells found in muscle tissue with platelet-derived growth factor receptor alpha (PDGFRα) serving as its general marker (15). Although FAPs contribute to fatty infiltration, it has been reported that transplantation of beige FAPs, a subpopulation of FAPs, suppressed fibrosis formation and fatty infiltration after rotator cuff tear (16, 17). A recent study identified MME (CD10)-positive FAPs as the key contributor to muscle fatty infiltration pathogenesis by single-nuclei RNA sequencing (7). These findings may suggest FAPs as future therapeutic targets to combat fatty expansion. Thus, it is important to study the effects of biological factors on fatty expansion via the heterogeneous populations of FAPs.

In this study, we evaluated the in vitro effect of FGF-8b supplementation on the differentiation of rotator cuff muscle-derived cells. We successfully utilized a method to separate FAPs and SCs from rotator cuff muscle tissue. Fibroblasts in the muscle tissues were shown to attach faster to collagen plates than muscle progenitor cells (MPCs) which proliferate

Author contributions: T.O. and C.T.L. designed research; T.O., H.-M.K., and B.T. performed research; T.O., H.-M.K., P.Y.M., and B.T. analyzed data; and T.O., H.-M.K., P.Y.M., and C.T.L. wrote the paper.

Reviewers: G.A., Northwestern University; and J.H., Johns Hopkins University School of Medicine.

Competing interest statement: The patent filings to disclose, entitled "Use of Fibroblast Growth Factor-8 for Tissue Regeneration" (Publication No.: WO/2022/150291).

[1]To whom correspondence may be addressed. Email: laurencin@uchc.edu.

This article contains supporting information online at https://www.pnas.org/lookup/suppl/doi:10.1073/pnas.2314585121/-/DCSupplemental.

Published December 26, 2023.

on Matrigel-coated plates (18). Therefore, the fast-attaching fibroblasts are expected to contain a high quantity of FAPs. Further, we analyzed the effect of FGF-8b supplementation on differentiation capability using FAPs-rich fibroblasts (FIBs) and SCs-rich MPCs. Finally, we studied the mechanisms involved, hypothesizing that ERK1/2 signaling would play an important role in determining fate decisions for adipogenesis and myogenesis.

Results

Separation of FIBs and MPCs from Rat Rotator Cuff Muscle. Two distinct cell populations were isolated from rotator cuff muscles (infraspinatus, supraspinatus, and subscapularis) and separated by repeated plating on two types of coated dishes, as described in Fig. 1*A*. These two cell populations showed different cell morphologies and metabolic activities (Fig. 1 *B*–*D*). Fast-attached fibroblasts (FIBs) showed a typical fibroblastic elongated cell shape, whereas MPCs showed more spherical and polygonal cell morphology. FIBs were positive for fibroblast markers (Vimentin and αSMA) and a marker for FAPs (PDGFRα) (Fig. 1 *E*–*G*). MPCs were positive for the satellite cell marker Pax7 and the myoprogenitor cell marker MyoD. Furthermore, MPCs were negative for the early myogenic differentiation marker Desmin, indicating that MPCs maintained an undifferentiated state (Fig. 1 *H*–*J*). Immunostaining for the FAPs and SCs marker showed successful separation of distinct cell populations between FIBs and MPCs (Fig. 1*K* and *SI Appendix*, Fig. S1).

FGF-8b Treatment Suppresses Adipogenesis and Tenogenesis of FIBs in a Dose-Dependent Manner. FGF-8b supplementation to adipogenic medium inhibited the formation of lipids with a dose-dependent trend (Fig. 2 *A* and *C*). This trend was consistent with our previous study using rat adipose-derived stem cells (14). In addition, immunofluorescent images showed myofiber formation and cell number were increased according to the FGF-8b concentration (Fig. 2*B*). Transcriptionally, FGF-8b supplementation showed a clear trend of downregulation for the adipogenic markers Pparg, Fabp4, Adipoq, and Lep (Fig. 2*D*). The expression of Pdgfra did not show statistically significant change up to 100 ng/mL of FGF-8b supplementation (Fig. 2*D*).

As for tenogenesis, FGF-8b supplementation suppressed tenascin C (Tnc) protein distribution in a dose-dependent manner *SI Appendix*, Fig. S2*A*). FGF-8b was also found to downregulate the expression of tenogenic markers (Scx, Tnmd, and Tnc) and tendon extracellular matrix proteins (Col1a1 and Col3a1, *SI Appendix*, Fig. S2*B*). Although both Col1a1 and Col3a1 mRNA expression was decreased at higher concentrations of FGF-8b, the alteration of the Col1a1/Col3a1 ratio was identified at 100 ng/mL (*SI Appendix*, Fig. S2*C*).

FGF-8b Supplementation Enhances the Myofiber Formation of MPCs in a Dose-Dependent Manner. MPCs were cultured in a myogenic medium with or without FGF-8b. FGF-8b was found to enhance the myofiber formation of MPCs as determined by immunostaining and qRT-PCR analysis (Fig. 3 *A*–*C*). Immunostaining of myosin heavy chain (MHC) showed increased myofiber formation in a dose-dependent manner (Fig. 3*B*). FGF-8b supplementation up-regulated the expression of both myogenic markers (MyoD and MyoG) and myogenic differentiation markers (Desmin and Tnnt1) at 10 ng/mL with a trend of upregulation with increasing FGF-8b concentrations (Fig. 3*C*).

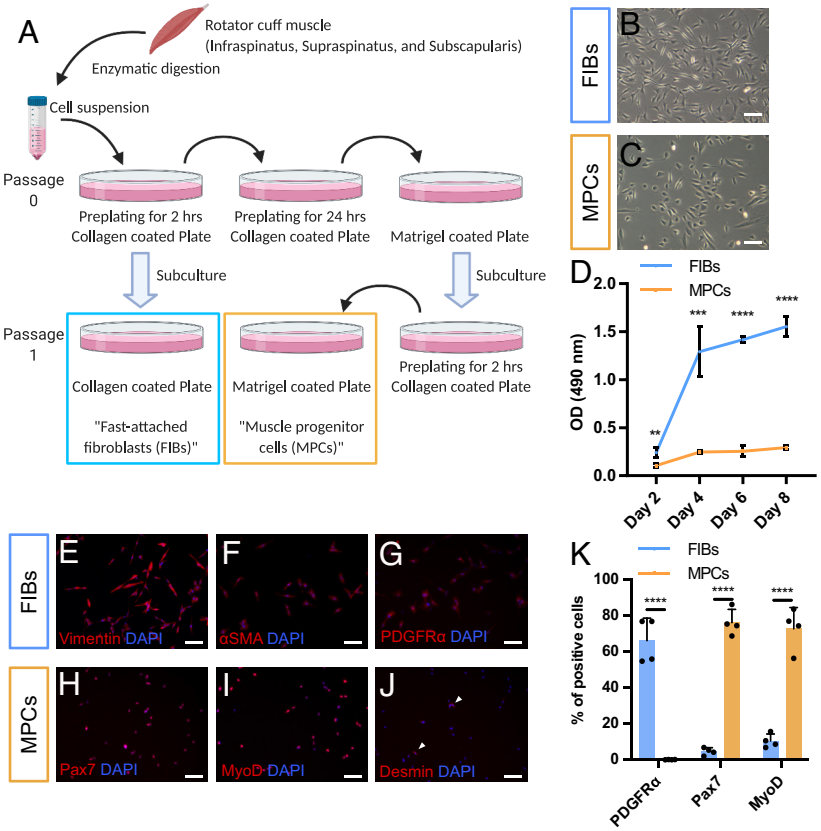

Fig. 1. Distinct cell population from rotator cuff muscle tissues. (*A*) Schematic images of the cell separation method. (*B* and *C*) Cell morphology of (*B*) FIBs and (*C*) MPCs at passage 2. (*D*) Metabolic activities between FIBs and MPCs measured by MTS assay ($n = 4$). (*E*–*G*) Immunostaining of FIBs. FIBs were positive for (*E*) Vimentin and (*F*) αSMA (fibroblast marker), and (*G*) PDGFRα (a marker of FAPs). (*H*–*J*) Immunostaining of MPCs. MPCs were positive for (*H*) Pax7 (SCs marker), (*I*) MyoD (myogenic progenitor marker), and negative for (*J*) Desmin (differentiated myoblast marker). (*K*) Quantification of FIBs and MPCs after staining with PDGFRα, Pax7, and MyoD antibodies. See also *SI Appendix*, Fig. S1. Ten different fields per samples were analyzed ($n = 4$). (Scale bar, 100 μm.)

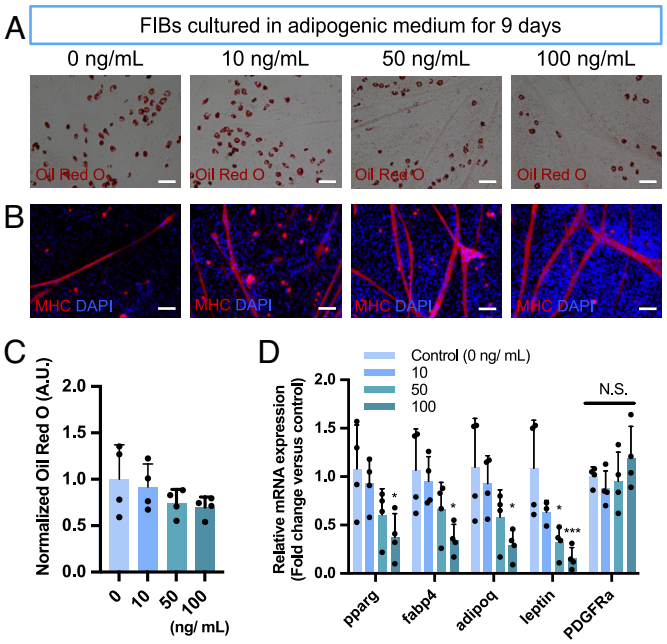

Fig. 2. FGF-8b suppresses adipogenesis of FIBs. (*A*) Representative images of the stained lipid droplets after 9 d of culture at the different concentrations of FGF-8b. (*B*) Representative fluorescent images stained with Myosin heavy chain (MHC) after 9 d of culture at the different concentrations of FGF-8b. (*C*) Quantification of the stained lipid droplets using the eluted Oil red O stain via measuring absorbance at 510 nm. The readings were normalized to background values of the adipogenic control condition (0 mg/mL) (n = 4). (*D*) mRNA expression of adipogenic marker genes (Pparg, Fabp4, Adipoq, and Lep) and the FAPs marker gene (Pdgfra). Data are expressed as fold change relative to the adipogenic control condition (0 mg/mL) (n = 4). (Scale bar, 100 μm.)

MPCs were also cultured in adipogenic or tenogenic mediums to evaluate the differentiation ability. MPCs did not undergo differentiation into adipocytes or tenocytes (*SI Appendix*, Fig. S3 *A* and *C*). On the other hand, MPCs differentiated into myocytes, and enhanced fiber formation was found with FGF-8b supplementation (*SI Appendix*, Fig. S3 *B* and *D*).

FGF Receptors Expression Is Altered by FGF-8b Supplementation. The expressions of four FGF receptors (FGFRs 1–4) that interact with FGF ligands were evaluated if those were autoregulated by FGF-8b supplementation. Note that endogenous mRNA expression of FGF-8 was not detected by qRT-PCR with or without FGF-8b supplementation. In both FIBs and MPCs, FGF-8b supplementation did not alter FGFRs expressions at day 1. In FIBs, FGF-8b supplementation induced reduced expression of FGFR2 and FGFR3 on day 9 (Fig. 4 *A*–*D*). FIBs showed higher expression of FGF receptors than MPCs, except for FGFR4.

Erk1/2 Pathway Is Responsible for the Proliferation and Differentiation of FIBs. Western blotting was performed for phosphorylated extracellular signal-related kinase (p-ERK1/2) and phosphorylated protein kinase B (p-AKT) expression in FIBs to identify the signaling pathways involved in adipogenic differentiation. FGF-8b supplementation showed increased p-ERK1/2 and slightly increased p-AKT levels in the FIBs (Fig. 5 *A*–*C*). The efficacies of the ERK1/2 (SCH772984) and AKT (LY294002) pathway inhibitors were confirmed by Western blotting analysis for phosphorylated ERK1/2 and AKT (Fig. 5 *A*–*C*). FGF-8b supplementation (+ FGF8, 100 ng/mL) promoted cell proliferation, whereas both ERK1/2 (iERK) and AKT (iAKT) inhibition suppressed cell proliferation compared to the control (– FGF8) under the normal growth medium condition (Fig. 5*D*). The effect of both inhibitors on adipogenesis was evaluated by Oil red O staining, suggesting the ERK inhibitor negated an effect of FGF-8b (Fig. 5 *E* and *G*). The quantification of DNA amount reflects cell number, demonstrating that the AKT inhibitor did not suppress cell proliferation in an adipogenic medium (Fig. 5*F*). The result of qRT-PCR showed no statistically significant difference between the – FGF8 control and iERK group for the adipogenic markers Pparg, Fabp4, Adipoq, and Lep (Fig. 5*H*). Although FGF-8b supplementation did not affect Pdgfra expression, ERK and AKT inhibitors had the opposite effect on Pdgfra gene expression.

Uncoupling protein 1 (Ucp1) expression is known to be induced by FGF-8b in preadipocytes (19). Contrary to previous studies, we found that FGF-8b supplementation did not induce detectable Ucp1 mRNA expression that was not detected at days 1 and 9. At day 9, iERK showed weak Ucp1 protein expression that was not found in the + FGF8 and iAKT groups (*SI Appendix*, Fig. S4).

Inhibition of Erk1/2 Pathway Affects the Survival of MPCs. FGF-8b supplementation showed an increased p-ERK1/2 level in MPCs but did not affect p-AKT level (Fig. 6 *A*–*C*). Therefore, the effect of ERK1/2 inhibitor on myogenic differentiation was investigated. Immunostaining of MHC showed that FGF-8b-treated MPCs had enhanced myofiber formation, while iERK-treated MPCs did not form myofibers (Fig. 6 *D* and *G*). DAPI staining and DNA quantification revealed a significant reduction of cell number in iERK-treated MPCs (Fig. 6 *D* and *F*). Consistent with this, Pax7 expression was also downregulated in iERK (Fig. 6 *E*, *H*, and *I*). As for the effect of FGF-8b on Pax7, Pax7-positive cell number were elevated (Fig. 6*H*). Transcriptionally, the expression of Pax7 in the + FGF8 group showed a trend of upregulation but did not show a statistically significant change compared to the – FGF8 control (Fig. 6*I*).

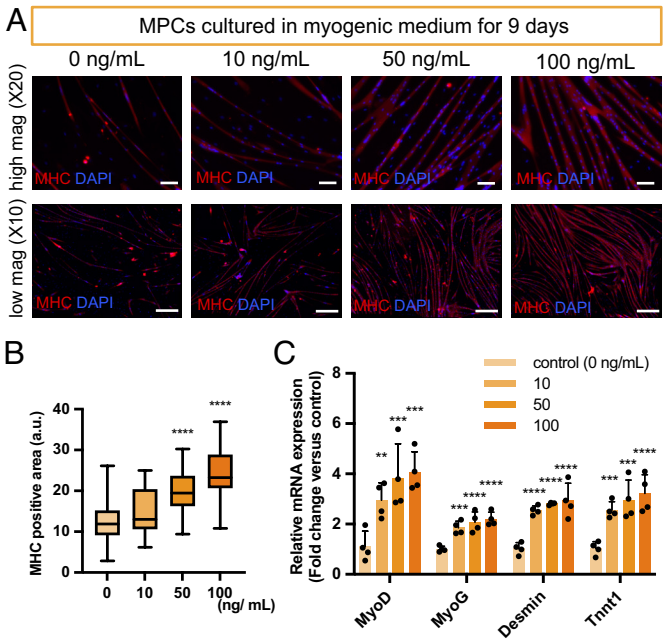

Fig. 3. FGF-8b enhances myogenesis of MPCs. (*A*) Representative fluorescent images stained with Myosin heavy chain (MHC) after 9 d of culture at the different concentrations of FGF-8b. (*B*) Quantification of MHC positive area. Ten different fields per sample were analyzed (n = 4). (*C*) mRNA expression of myogenic markers (MyoD, MyoG, Desmin, and Tnnt1). Data are expressed as fold change relative to the myogenic control condition (0 mg/mL) (n = 4). Scale bar: 100 μm (high magnification, upper lane) and 2 mm (low magnification, lower lane).

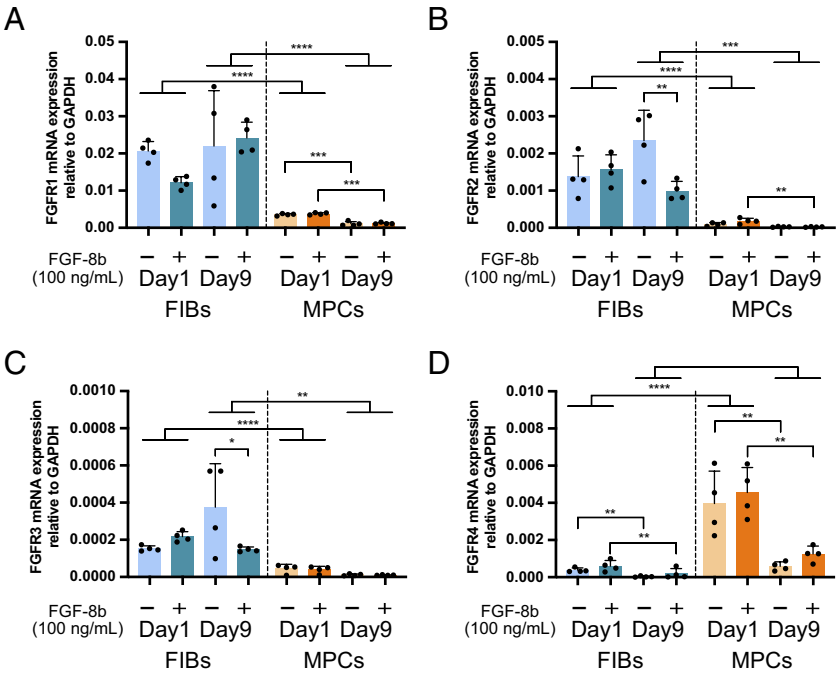

Fig. 4. The alteration of FGF receptor expression in FIBs and MPCs. Relative mRNA expression of (*A*) FGFR1, (*B*) FGFR2, (*C*) FGFR3, and (*D*) FGFR4. Gapdh was used as the internal control against which the mRNA expressions of FGF receptors were normalized (n = 4).

Discussion

Muscle degeneration, including fat accumulation, fibrosis, and muscle atrophy, is a common finding following rotator cuff tears (3, 20–22). We previously reported that FGF-8b supplementation altered mesenchymal stem cell fate by suppressing adipogenesis and enhancing myogenesis (14). In this study, we hypothesized that this feature might be suitable for treating muscle degeneration. Here, we evaluated key cell populations involved in fatty infiltration and subsequent degeneration of muscle tissue in rotator cuff repair. The effects of FGF-8b supplementation on cell fate decision using rotator cuff muscle-derived cells were recapitulated. We also identified ERK signaling as the mechanism of action of FGF-8b in these specific cell populations (Fig. 7).

Fatty expansion and muscle atrophy are considered independently associated processes (23). Since skeletal muscle is highly heterogeneous, functional crosstalk is crucial for muscle repair (24). While satellite cells (SCs) are the primary source of myoblasts in response to an injury (25, 26), FAPs have been identified as the primary source of fibrosis and fatty expansion in skeletal muscle in the rodent models (5, 21). It should be noted that whether FAPs contribute to human muscle degeneration following injury still needs to be studied (27–29). In addition, most of the small animal models of rotator cuff tear are acute or subacute (30–33). These models required a nerve injury to cause severe muscle degeneration, including fatty infiltration, which limits the clinical relevance to human cases. However, we recently established a chronic rotator cuff tear model demonstrating that rodents also underwent fatty infiltration and fibrosis formation without the resection of nerve (34). Therefore, we utilized a rat model and applied a simple method to separate cell populations from the rotator cuff muscle to analyze rotator cuff cell population responses to FGF-8b.

It has been reported that preplating muscle-derived cells on a collagen-coated plate before plating on a Matrigel-coated plate can eliminate the epithelial or fibroblastic cells (18). By using a specific coating and repeated plating procedure, we successfully separated the FAPs-rich cell population (FIBs) and SCs-rich cell population (MPCs) from tissue samples (Fig. 1). These two cell populations showed different cell shapes (Fig. 1 *B* and *C*), metabolic activity (Fig. 1*D*), marker protein expression (Fig. 1*K*), and differentiation ability (*SI Appendix*, Fig. S3). Lower metabolic activity has been reported in quiescent SCs (35). In addition, the early differentiation marker, Desmin, was less found in MPCs (Fig. 1*J*). These suggest the majority of isolated MPCs were in an undifferentiated state. Although the purity is less than that derived from fluorescence-activated cell sorting (FACS) [e.g., 96.6 ± 4.2% Pax7-positive SCs obtained from YFP knock-in-mouse (36)], this more facile method can be used to understand differentiation potential and gene expression among these different cell types without using transgenic animals or antibody staining. However, it should be mentioned that crude cell separation caused heterogeneous cell population, which was one of our limitations in this study.

Ucp1 is a characteristic of differentiated brown adipocytes and is associated with heat production (37). FGF-8b has been reported to induce ucp1 expression in white and brown mouse preadipocytes (19, 38). Transplantation of FACS-sorted Ucp1-positive FAPs has been shown to improve muscle function after rotator cuff injury in rat models (16, 17). However, the present study showed no evidence of Ucp1 expression induced by FGF-8b supplementation (*SI Appendix*, Fig. S4). We also did not detect ucp1 mRNA expression at any time point. One study showed that FAPs could potentially differentiate into ucp1-expressing adipocytes (39). Therefore, the effect of FGF-8b on Ucp1-positive FAPs is of interest.

To understand the signaling pathway, studying the FGF ligand and receptor complex is essential (40). Autoregulation often controls receptor expression to modulate the intracellular signaling pathway (41, 42). In the present study, we evaluated the expression pattern of FGFR1–4 at two-time points in FIBs and MPCs (Fig. 4). In both FIBs and MPCs populations, autoregulatory effects were not observed at an early time point. Although FGF-8b supplementation did not show statistically significant changes, FGF-8b showed a trend of downregulation of FGFR1 expression in FIBs.

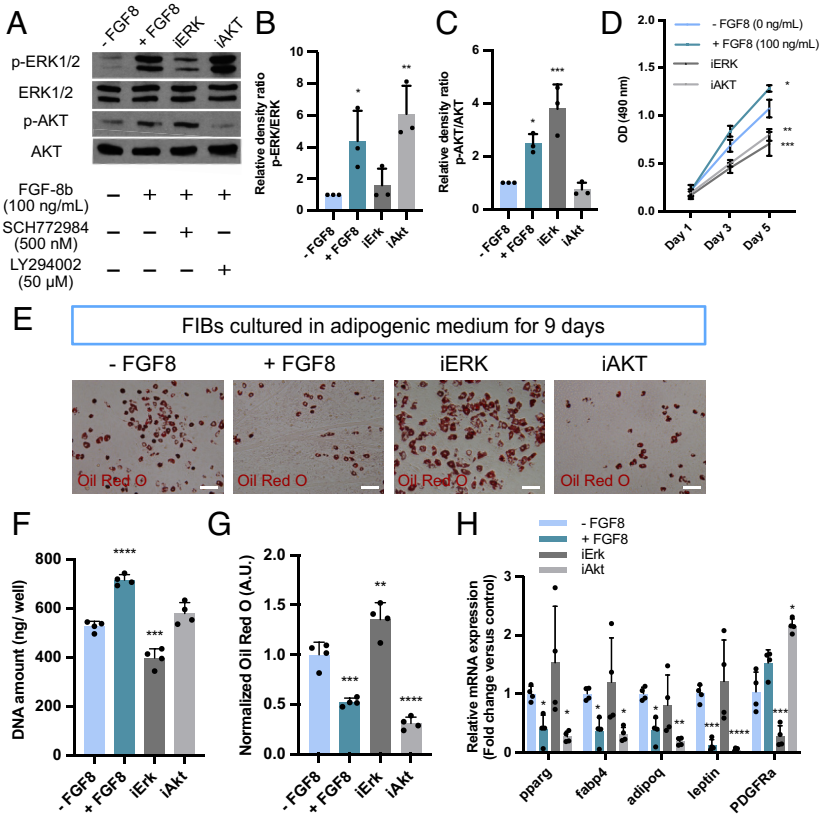

Fig. 5. ERK1/2 pathway is responsible for the proliferation and FGF8-driven differentiation control of FIBs. (*A*) The expression of p-ERK1/2, ERK1/2, p-AKT, and AKT in FIBs analyzed by Western blot; the plus sign represents the material was added to the medium, and the minus sign indicates the material was absent from the culture medium. (*B* and *C*) The density of each band was quantified by ImageJ software for (*B*) p-ERK1/2 and (*C*) p-AKT, and the relative density ratio of each protein was calculated accordingly ($n = 3$). (*D*) The effect of FGF-8b, ERK1/2 inhibitor, and AKT inhibitor on cell proliferation grown in growth medium measured by MTS assay ($n = 4$). (*E*) Representative images of the stained lipid droplets after 9 d of culture. (*F*) DNA quantification of FIBs cultured in adipogenic medium ($n = 4$). (*G*) Quantification of the stained lipid droplets using the eluted Oil red O stain via measuring absorbance at 510 nm. The readings were normalized to background values of the − FGF8 group ($n = 4$). (*H*) mRNA expression of adipogenic marker genes (Pparg, Fabp4, Adipoq, and Lep) and the FAPs marker gene (Pdgfra). Data are expressed as fold change relative to the adipogenic control condition (− FGF8) ($n = 4$). (Scale bar, 100 μm.)

FGFR1 was a key regulator of early adipogenic events that binds to FGF1 and/or FGF2 in a human preadipocyte (43). FGFR4 is known to be highly expressed in satellite cells (44). Nine days after cultivation in myogenic medium, FGF-8b supplementation showed a trend of higher FGFR4 expression compared to the control, which was not a statistically significant difference (Fig. 4*D*). In addition, our results demonstrated that Pax7 expression was not significantly elevated, but an increase in Pax7-positive cell number was found (Fig. 6 *H* and *I*). Activated SCs withdraw irreversibly from the cell cycle and undergo myogenic differentiation, which leads to a shortage of stem cells in long-term myogenic culture conditions (45). Differentiated myofibers are also not retained in long-term 2D culture due to unstable attachment of myofibers or the contamination of fibroblasts, leading to myofiber detachment within approximately 1 wk (29, 46). Our results suggested that FGF-8b facilitated the maintenance of satellite stem cells by promoting self-renewal, which supplies myogenic differentiating cells continuously. A recent study suggested that FGFR4-positive cells possess a higher regenerative capacity among the iPSC-derived heterogeneous MPC population (47). Therefore, FGF-8b supplementation may contribute to pooling a highly regenerative satellite cell population. However, further study focused on autoregulation, such as autophosphorylation and dimerization, needs to be addressed to understand FGF ligand–receptor regulation.

Here, we demonstrated that FGF-8b supplementation suppressed adipogenesis dose-dependently (Fig. 2). Furthermore, our results showed that inhibition of the ERK1/2 signaling pathway negated the effect of FGF-8b and promoted adipogenesis (Fig. 5 *C*, *E*, and *F*), contrary to previous reports on the role of ERK signaling in adipogenesis. Classically, ERK signaling is thought to promote adipogenesis (48). Mathes et al. demonstrated that FGF-2 stimulated intramuscular adipogenesis in aged human skeletal muscle through the ERK signaling pathway (49). On the other hand, there are studies showing that FGF-8b has the ability to downregulate adipogenic differentiation in various cell types, such as mouse preadipocytes, rat adipose-derived stem cells, and rat FAPs (14, 19). Similarly, our result demonstrated that the upregulation of ERK1/2 signaling significantly affected satellite cell number and myofiber formation (Fig. 6), while it has been reported that ERK1/2 inhibition promotes myotube growth via CaMKII activation of mouse SCs (50). Long-term treatment of ERK1/2 inhibitor may affect SCs survival, although our treatment of ERK1/2 inhibitor was half the dose of the previous study. These contrary results may be due to ligand-specific unique features. Therefore, FGF-8b is a potential alternative to FGF-2 or, in combination, to enhance myogenesis while potentially suppressing the pro-adipogenic effect of FGF-2.

AKT is another important FGF signaling pathway. It has been reported that FGF2-induced PI3K/Akt signaling promoted cell proliferation and adipogenic differentiation of human adipose-derived stem cells (51). In the present study, inhibition of AKT signaling showed the trend of downregulation of adipogenesis compared to the + FGF-8b group but did not show statistically significant changes (Fig. 5 *E* and *F*). ERK1/2 and AKT inhibition suppressed cell

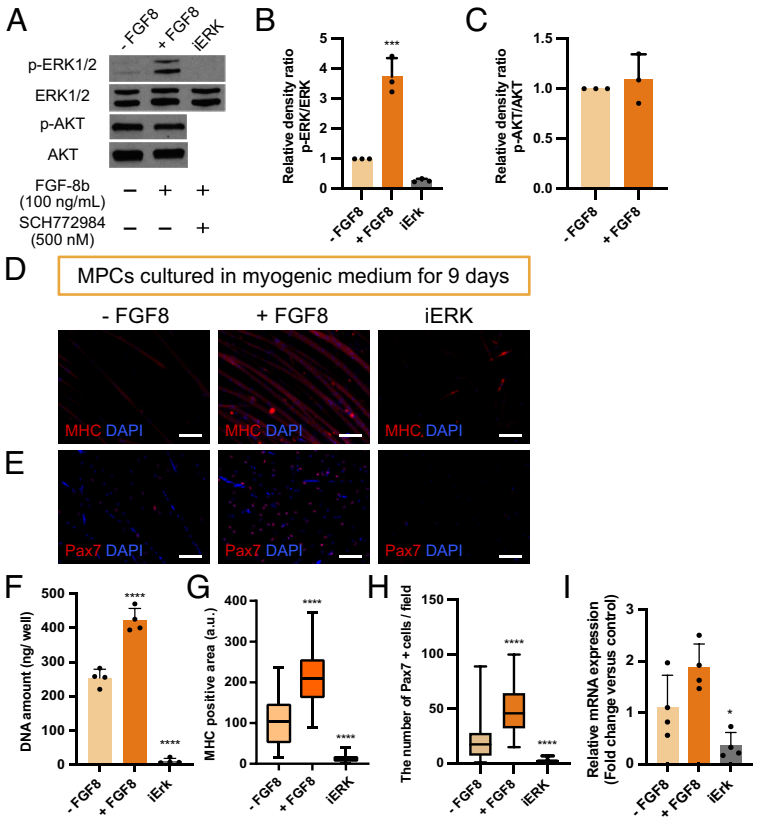

Fig. 6. Inhibition of Erk1/2 pathway induces the reduction of MPCs. (*A*) The expression of p-ERK1/2, ERK1/2, p-AKT, and AKT in MPCs analyzed by Western blot; the plus sign represents the material was added to the medium, and the minus sign indicates the material was absent from the culture medium. (*B* and *C*) The density of each band was quantified by ImageJ software for (*B*) p-ERK1/2 and (*C*) p-AKT, and the relative density ratio of each protein was calculated accordingly (n = 3). (*D*) Representative fluorescent images stained with Myosin heavy chain (MHC) after 9 d of culture. (*E*) Representative fluorescent images stained with Pax7 after 9 d of culture. (*F*) DNA quantification of MPCs cultured in myogenic medium (n = 4). (*G*) Quantification of MHC positive area. Ten different fields per sample were analyzed (n = 4). (*H*) Quantification of Pax7 positive cells/field. Ten different fields per sample were analyzed (n = 4). (*I*) mRNA expression of Pax7. Data are expressed as fold change relative to the myogenic control condition (− FGF8) (n = 4). (Scale bar, 100 μm.)

proliferation in the growth medium, but AKT inhibition did not suppress cell proliferation in the adipogenic medium, suggesting that cells did not undergo adipogenic differentiation and continued to proliferate (Fig. 5 *B* and *D*). Lastly, AKT inhibition up-regulated Pdgfra expression, which is the marker for FAPs (Fig. 5*F*). It is unclear whether the AKT signaling pathway is involved in FGF-8b administration during adipogenic differentiation; however, AKT signaling may contribute to the maintenance of FAPs.

Fibrosis is one of the unwanted consequences after rotator cuff injury (2, 21, 52). Since the tendon is prone to form fibrotic scars during regeneration, it is crucial to avoid excessive scar tissue (53). Although our result showed tenogenesis suppression, the alteration of collagen type I/III ratio may contribute to remodeling the ECM composition remodeling (*SI Appendix*, Fig. S2) (54). Inhibition of differentiation into tendon cells by FGF-8b may affect the outcome of in vivo studies. Therefore, it may be necessary to develop intramuscular localization without disturbing tenogenic regeneration for the therapeutic use of FGF-8b.

Overall, we evaluated the effects of FGF-8b on reducing fat accumulation and enhancing myofiber formation in vitro. The ERK1/2 signaling pathway possesses important roles in adipogenesis of FIBs and cell survival of MPCs. These results support the potential use of FGF-8b to treat muscle degeneration. However, the impact of the source tissue (age, sex, etc.) on the isolation of cell populations and the response to the growth factor needs to be evaluated in the future. Further studies are also needed to determine whether this mechanism of action is conserved in human cells. In addition, the efficacy of FGF-8b in vivo and the appropriate growth factor delivery systems need to be addressed. Recent studies from our group have shown that electroconductive matrices can be used to treat muscle degeneration after rotator cuff injury (34, 55, 56). In addition, the use of graphene oxide has been widely explored as a growth factor delivery carrier (57–59). The combinatorial use of matrices and FGF-8b may provide a new platform for treating muscle degeneration which can be investigated in future studies (60). In

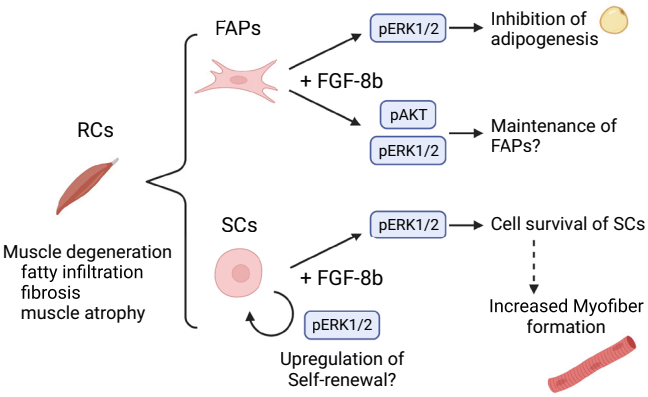

Fig. 7. Schematic image of cell fate control in FIBs and MPCs via FGF-8b supplementation. FIBs showed decreased adipogenesis of FAPs under FGF-8b supplementation via ERK1/2 pathway. MPCs showed up-regulated myofiber formation under FGF-8b supplementation. ERK1/2 pathway may be involved in the cell survival of satellite stem cells (SCs).

conclusion, the findings of these studies demonstrate the powerful potential of FGF-8b for rotator cuff repair by altering the fate of muscle undergoing degeneration.

Materials and Methods

Reagents. Recombinant growth factors were obtained from R&D Systems: human fibroblast growth factor 2 (FGF-2, 233-FB), FGF-8b (423-F8), platelet-derived growth factor-BB (PDGF-BB, 220-BB), and mouse growth differentiation factor 6 (GDF-6, 855-G6). Recombinant human Insulin (rh-insulin, I2643) was obtained from Millipore Sigma. Erk1/2 pathway inhibitor (SCH772984) and AKT pathway inhibitor (LY294002) were obtained from Cayman chemicals. FGF-8b (10, 50, 100 ng/mL), 500 nM of SCH772984, and 50 μM of LY294002 were supplemented in the culture medium.

FIBs and MPCs Isolation and Culture. Experiments were performed on adult Sprague–Dawley rats (Charles River Laboratories, Inc.) that were killed by CO_2 inhalation followed by neck dislocation in accordance with the experimental guidelines and regulations approved by University of Connecticut Health Center Institutional Animal Care and Use Committee (IACUC)-approved protocol. Additionally, cell isolation was done following the institutional IACUC-approved protocol. We collected biological replicates from different animals. Two distinct cell populations (FIBs and MPCs) were isolated from Sprague-Dawley rats (sex: male, age: 6 to 7 wk, weight: 200 to 350 g), as described in Fig. 1*A*. Rotator cuff muscles (infraspinatus, supraspinatus, and subscapularis) were harvested and minced. Tissues were digested in collagenase type I (0.2%, w/v; Gibco) and dispase II (0.2%, w/v; Sigma) in high glucose DMEM (Gibco) and agitated at 37 °C for 45 min. The cell suspension was filtered through a 100-μm filter to remove solid aggregates. Subsequently, the cells were plated on a collagen-coated plate containing high glucose DMEM supplemented with 20% fetal bovine serum (FBS), 1% penicillin-streptomycin (pen/strep), and 25 ng/mL of recombinant human FGF-2 (growth medium; GM), incubated for 2 h in a 37 °C, 5% CO_2 incubator. After 2 h of incubation, the supernatant was transferred to another collagen-coated plate. The remaining attached cells on the initial collagen-coated plate were incubated in GM to keep the FIBs (Fig. 1*A*). To isolate MPCs, the transferred supernatant was further incubated for 24 h to allow fibroblasts to attach to the new collagen-coated plate. Subsequently, the supernatant was transferred to a Matrigel-coated plate. At the time of subculture, MPCs were preplated for 2 h on a collagen-coated plate to eliminate fibroblasts, then transferred to a Matrigel-coated plate at passage 1. The culture medium was changed every 2 d. All in vitro studies were performed at passage 2.

Multilineage Differentiation Induction. To induce adipogenic differentiation, FIBs and MPCs were seeded at a density of 600 cells/μL and cultured for 3 d in high glucose DMEM supplemented with 10% Horse serum, 1% pen/strep, 10 μg/mL rh-insulin, I μM dexamethasone, 0.1 mM indomethacin, and 0.5 mM 3-isobutyl-1-methylxanthine (Adipogenic induction medium). Then, FIBs and MPCs were further cultured for 6 d in high glucose DMEM supplemented with 10% Horse serum, 1% pen/strep, and 10 μg/mL rh-insulin (Adipogenic maintenance medium). Adipogenic differentiation was confirmed by staining with Oil-Red O. The cultures were fixed in 10% formalin for 10 min and then incubated for 20 min in Oil Red O solution. After qualitative analysis by microscopy, the stain was eluted with 100% isopropanol for 10 min and analyzed at 518 nm absorbance.

To induce tenogenic differentiation, FIBs and MPCs were seeded at a density of 600 cells/μL and cultured for 9 d in high glucose DMEM supplemented with 10% FBS, 1% pen/strep, 50 ng/mL GDF-6, and 10 ng/mL PDGF-BB (Tenogenic medium) as previously described (14).

To induce myogenic differentiation, FIBs and MPCs were seeded at a density of 600 cells/μL and cultured for 9 d in high glucose DMEM supplemented with 5% horse serum and 1% pen/strep (Myogenic medium). During the differentiation induction, the culture medium was changed every 3 d with/without FGF-8b supplementation.

MTS Assay. Cell metabolic activity and proliferation were assessed using the CellTiter® 96 AQueous nonradioactive cell proliferation assay (Promega) as previously described (14). Briefly, cells were washed with PBS, then MTS reagent in a ratio of 5:1 (medium: MTS) was added to each well. The plates were incubated for 1 h at 37 °C. The absorbance of the resulting solution was read at 490 nm using a microplate reader.

DNA Quantification. DNA was isolated and quantified using the Quant-iT PicoGreen dsDNA assay kit (Invitrogen) as previously described (14). Briefly, cell lysates were collected and mixed with the Quant-iT PicoGreen reagent, measured via spectrophotometry at 535 nm with excitation at 485 nm. DNA content was quantified using a standard curve.

Quantitative Real-Time PCR (qRT-PCR). Quantitative real-time PCR was performed as previously described (14). Total RNA was isolated using the RNeasy Mini Kit (Qiagen, Alameda, California) according to the manufacturer's instructions. Then, 1 to 2 μg of total RNA was reverse-transcribed to cDNA by using RNA to cDNA EcoDry Premix (Clontech) in a total volume of 20 μL. Taqman predesigned primers (Thermo Fisher Scientific) (*SI Appendix*, Table S1, including Fgf8 and Ucp1 that were not detected in this study) were used for qRT-PCR, and the signal was detected by the CFX Connect Real-Time System (Bio-Rad). The threshold cycle values of target genes were standardized against Gapdh expression using the ΔCq method (Fig. 4). Except for Fig. 4, gene expressions were further normalized to the expression in the control culture. The fold change in expression was calculated using the ΔΔCq comparative threshold cycle method. All qRT-PCRs were run in quadruplicate with three technical replicates.

Western Blotting. After 2 h of treatment with/without inhibitors, the cells were collected and lysed in CellLytic M (Millipore Sigma) and protease inhibitor (Thermo Fisher Scientific) to obtain the total protein. The protein concentration was determined by the BCA protein assay kit (Thermo Fisher Scientific). Equal amounts of protein (5 μg) were separated by 10% SDS-PAGE and transferred onto a 0.2 mm Nitrocellulose Membrane. Then, the membranes were blocked by EveryBlot blocking buffer (BioRad) and probed with primary antibodies at 4 °C overnight, followed by incubation with HRP-conjugated secondary antibodies at room temperature for 30 min. Primary and secondary antibodies used in this study were listed in *SI Appendix*, Table S2. The SuperSignal™ West Pico PLUS Chemiluminescent Substrate (Thermo Fisher Scientific) was used for detection, and CL-XPosure Film (Thermo Fisher Scientific) was used for exposure of the membranes. Full blot images were shown in *SI Appendix*, Fig. S5. The relative density of the bands was quantified by ImageJ software.

Immunofluorescence. Immunofluorescence staining was performed as previously described (14). Briefly, cells were rinsed with PBS, fixed with 4% paraformaldehyde in PBS for 20 min at room temperature, and permeabilized with 0.1% Triton X 100 for 10 min at room temperature. Then, cells were blocked by 1% bovine serum albumin (Sigma) for 1 h at room temperature and incubated with primary antibodies overnight at 4 °C. Thereafter, cells were rinsed thrice with PBS and incubated with secondary antibodies for 2 h at room temperature in the dark. Primary and secondary antibodies used in this study were listed in *SI Appendix*, Table S2. All stained samples were examined under a Leica DMi8 inverted microscope (Leica Microsystems). Cell numbers were manually counted on 10 images per well. To calculate the MHC positive stained area, images were converted to 8-bit, then Huang threshold (B&W) with the dark background was applied, and the area was measured using the ImageJ software.

Statistical Analysis. GraphPad Prism 7 (GraphPad Software) was used for statistical analysis and graph design. Results were expressed as the mean values ± SD. Comparisons between two groups were performed with the unpaired Student's *t* test. Comparisons of more than two groups were performed with One-way ANOVA with Dunnett's post hoc test or Two-way ANOVA with Šidák's tests. Differences were considered significant if the *P*-value was <0.05. Statistical significance was shown with $*P < 0.05$, $**P < 0.01$, $***P < 0.001$, and $****P < 0.0001$.

Data, Materials, and Software Availability. All study data are included in the article and/or *SI Appendix*.

ACKNOWLEDGMENTS. This research was supported by funding from NIH DP1AR068147. Biorender.com was used for the illustration.

Author affiliations: [a]The Cato T. Laurencin Institute for Regenerative Engineering, University of Connecticut, Storrs, CT 06269; [b]Raymond and Beverly Sackler Center for Biomedical, Biological, Physical, and Engineering Sciences, University of Connecticut Health Center, Farmington, CT 06030; [c]Department of Orthopedic Surgery, University of Connecticut Health Center, Farmington, CT 06030; [d]Department of Biomedical Engineering, University of Connecticut, Storrs, CT 06269; [e]Department of Materials Science and Engineering, University of Connecticut, Storrs, CT 06269; and [f]Department of Chemical and Biomolecular Engineering, University of Connecticut, Storrs, CT 06269

1. B. R. Kuzel, S. Grindel, R. Papandrea, D. Ziegler, Fatty infiltration and rotator cuff atrophy. *J. Am. Acad. Orthop. Surg.* **21**, 613–623 (2013).
2. L. Osti, M. Buda, A. Del Buono, Fatty infiltration of the shoulder: Diagnosis and reversibility. *Muscles, Ligaments Tendons J.* **3**, 351 (2013).
3. T. Thangarajah *et al.*, Supraspinatus detachment causes musculotendinous degeneration and a reduction in bone mineral density at the enthesis in a rat model of chronic rotator cuff degeneration. *Shoulder Elb.* **9**, 178–187 (2017).
4. N. Saveh-Shemshaki, L. S. Nair, C. T. Laurencin, Nanofiber-based matrices for rotator cuff regenerative engineering. *Acta Biomater.* **94**, 64–81 (2019).
5. A. Uezumi *et al.*, Fibrosis and adipogenesis originate from a common mesenchymal progenitor in skeletal muscle. *J. Cell Sci.* **124**, 3654–3664 (2011).
6. O. Agha *et al.*, Rotator cuff tear degeneration and the role of fibro-adipogenic progenitors. *Ann. N. Y. Acad. Sci.* **1490**, 13–28 (2021).
7. G. Fitzgerald *et al.*, MME+ fibro-adipogenic progenitors are the dominant adipogenic population during fatty infiltration in human skeletal muscle. *Commun. Biol.* **6**, 111 (2023).
8. A. P. Valencia *et al.*, Fatty infiltration is a prognostic marker of muscle function after rotator cuff tear. *Am. J. Sports Med.* **46**, 2161–2169 (2018).
9. L. E. Tellier *et al.*, Localized SDF-1α delivery increases pro-healing bone marrow-derived cells in the supraspinatus muscle following severe rotator cuff injury. *Regen. Eng. Transl. Med.* **4**, 92–103 (2018).
10. A. Prabhath *et al.*, Pegylated insulin-like growth factor-1 biotherapeutic delivery promotes rotator cuff regeneration in a rat model. *J. Biomed. Mater. Res., Part A* **110**, 1356–1371 (2022).
11. C. Wang, Q. Hu, W. Song, W. Yu, Y. He, Adipose stem cell-derived exosomes decrease fatty infiltration and enhance rotator cuff healing in a rabbit model of chronic tears. *Am. J. Sports Med.* **48**, 1456–1464 (2020).
12. A. Prabhath, V. N. Vernekar, E. Sanchez, C. T. Laurencin, Growth factor delivery strategies for rotator cuff repair and regeneration. *Int. J. Pharm.* **544**, 358–371 (2018).
13. H. N. Wang, X. Rong, L. M. Yang, W. Z. Hua, G. X. Ni, Advances in stem cell therapies for rotator cuff injuries. *Front. Bioeng. Biotechnol.* **10**, 778 (2022).
14. T. Otsuka, P. Y. Mengsteab, C. T. Laurencin, Control of mesenchymal cell fate via application of FGF-8b in vitro. *Stem Cell Res.* **51**, 102155 (2021).
15. A. Uezumi *et al.*, Identification and characterization of PDGFR + mesenchymal progenitors in human skeletal muscle. *Cell Death Dis.* **5**, e1186 (2014).
16. C. Lee *et al.*, Beige fibro-adipogenic progenitor transplantation reduces muscle degeneration and improves function in a mouse model of delayed repair of rotator cuff tears. *J. Shoulder Elb. Surg.* **29**, 719–727 (2020).
17. C. Lee *et al.*, Beige FAPs transplantation improves muscle quality and shoulder function after massive rotator cuff tears. *J. Orthop. Res.* **38**, 1159–1166 (2020).
18. A. Shahini *et al.*, Efficient and high yield isolation of myoblasts from skeletal muscle. *Stem Cell Res.* **30**, 122–129 (2018).
19. S. Westphal *et al.*, Fibroblast growth factor 8b induces uncoupling protein 1 expression in epididymal white preadipocytes. *Sci. Rep.* **9**, 1–11 (2019).
20. Y. S. Lee, J. Y. Jeong, C. D. Park, S. G. Kang, J. C. Yoo, Evaluation of the risk factors for a rotator cuff retear after repair surgery. *Am. J. Sports Med.* **45**, 1755–1761 (2017).
21. X. Liu *et al.*, Investigating the cellular origin of rotator cuff muscle fatty infiltration and fibrosis after injury. *Muscles, Ligaments Tendons J.* **6**, 6–15 (2016).
22. K. S. Washington, N. S. Shemshaki, C. T. Laurencin, The role of nanomaterials and biological agents on rotator cuff regeneration. *Regen. Eng. Transl. Med.* **7**, 440–449 (2021).
23. J. J. Barry, D. A. Lansdown, S. Cheung, B. T. Feeley, C. B. Ma, The relationship between tear severity, fatty infiltration, and muscle atrophy in the supraspinatus. *J. Shoulder Elb. Surg.* **22**, 18–25 (2013).
24. B. Biferali, D. Proietti, C. Mozzetta, L. Madaro, Fibro-adipogenic progenitors cross-talk in skeletal muscle: The social network. *Front. Physiol.* **10**, 1074 (2019).
25. F. Relaix, P. S. Zammit, Satellite cells are essential for skeletal muscle regeneration: The cell on the edge returns centre stage. *Development* **139**, 2845–2856 (2012).
26. P. Feige, C. E. Brun, M. Ritso, M. A. Rudnicki, Orienting muscle stem cells for regeneration in homeostasis, aging, and disease. *Cell Stem Cell* **23**, 653–664 (2018).
27. O. Contreras, F. M. V. Rossi, M. Theret, Origins, potency, and heterogeneity of skeletal muscle fibro-adipogenic progenitors–Time for new definitions. *Skelet. Muscle* **11**, 16 (2021).
28. C. Moratal *et al.*, IL-1β- and IL-4-polarized macrophages have opposite effects on adipogenesis of intramuscular fibro-adipogenic progenitors in humans. *Sci. Rep.* **8**, 17005 (2018).
29. Q. Mao *et al.*, Tension-driven multi-scale self-organisation in human iPSC-derived muscle fibers. *eLife* **11**, e76649 (2022).
30. R. Bell, P. Taub, P. Cagle, E. L. Flatow, N. Andarawis-Puri, Development of a mouse model of supraspinatus tendon insertion site healing. *J. Orthop. Res.* **33**, 25–32 (2015).
31. T. Kanazawa *et al.*, Histomorphometric and ultrastructural analysis of the tendon–bone interface after rotator cuff repair in a rat model. *Sci. Rep.* **6**, 33800 (2016).
32. Y. Sasaki *et al.*, Histological analysis and biomechanical evaluation of fatty infiltration after rotator cuff tear and suprascapular nerve injury in a rat model. *J. Orthop. Sci.* **23**, 834–841 (2018).
33. H. Shirasawa *et al.*, Inhibition of PDGFR signaling prevents muscular fatty infiltration after rotator cuff tear in mice. *Sci. Rep.* **7**, 41552 (2017).
34. N. S. Shemshaki *et al.*, Muscle degeneration in chronic massive rotator cuff tears of the shoulder: Addressing the real problem using a graphene matrix. *Proc. Natl. Acad. Sci. U.S.A.* **119**, e2208106119 (2022).
35. P. Rocheteau, B. Gayraud-Morel, I. Siegl-Cachedenier, M. A. Blasco, S. Tajbakhsh, A subpopulation of adult skeletal muscle stem cells retains all template DNA strands after cell division. *Cell* **148**, 112–125 (2012).
36. Y. Kitajima, Y. Ono, Visualization of PAX7 protein dynamics in muscle satellite cells in a YFP knock-in-mouse line. *Skelet. Muscle* **8**, 26 (2018).
37. B. Cannon, J. Nedergaard, Brown adipose tissue: Function and physiological significance. *Physiol. Rev.* **84**, 277–359 (2004).
38. T. Gantert *et al.*, Fibroblast growth factor induced Ucp1 expression in preadipocytes requires PGE2 biosynthesis and glycolytic flux. *FASEB J.* **35**, e21572 (2021).
39. T. Gorski, S. Mathes, J. Krützfeldt, Uncoupling protein 1 expression in adipocytes derived from skeletal muscle fibro/adipogenic progenitors is under genetic and hormonal control. *J. Cachexia, Sarcopenia Muscle* **9**, 384–399 (2018).
40. V. P. Eswarakumar, I. Lax, J. Schlessinger, Cellular signaling by fibroblast growth factor receptors. *Cytokine Growth Factor Rev.* **16**, 139–149 (2005).
41. N. N. Mott, W. C. J. Chung, P. S. Tsai, T. R. Pak, Differential fibroblast growth factor 8 (FGF8)-mediated autoregulation of its cognate receptors, Fgfr1 and Fgfr3, in neuronal cell lines. *PLoS ONE* **5**, e10143 (2010).
42. W. T. Lai, V. Krishnappa, D. G. Phinney, Fibroblast growth factor 2 (Fgf2) inhibits differentiation of mesenchymal stem cells by inducing Twist2 and Spry4, blocking extracellular regulated kinase activation, and altering fgf receptor expression levels. *Stem Cells* **29**, 1102–1111 (2011).
43. C. H. Widberg *et al.*, Fibroblast growth factor receptor 1 is a key regulator of early adipogenic events in human preadipocytes. *Am. J. Physiol.: Endocrinol. Metab.* **296**, 121–131 (2009).
44. S. Kastner, M. C. Elias, A. J. Rivera, Z. Yablonka-Reuveni, Gene expression patterns of the fibroblast growth factors and their receptors during myogenesis of rat satellite cells. *J. Histochem. Cytochem.* **48**, 1079–1096 (2000).
45. K. Walsh, H. Perlman, Cell cycle exit upon myogenic differentiation. *Curr. Opin. Genet. Dev.* **7**, 597–602 (1997).
46. A. Benedetti *et al.*, A novel approach for the isolation and long-term expansion of pure satellite cells based on ice-cold treatment. *Skelet. Muscle* **11**, 7 (2021).
47. M. Nalbandian *et al.*, Single-cell RNA-seq reveals heterogeneity in hiPSCderived muscle progenitors and E2F family as a key regulator of proliferation. *Life Sci. Alliance* **5**, e202101312 (2022).
48. D. Prusty, B. H. Park, K. E. Davis, S. R. Farmer, Activation of MEK/ERK signaling promotes adipogenesis by enhancing peroxisome proliferator-activated receptor γ (PPARγ) and C/EBPα gene expression during the differentiation of 3T3-L1 preadipocytes. *J. Biol. Chem.* **277**, 46226–46232 (2002).
49. S. Mathes *et al.*, FGF-2–dependent signaling activated in aged human skeletal muscle promotes intramuscular adipogenesis. *Proc. Natl. Acad. Sci. U.S.A.* **118**, e2021013118 (2021).
50. T. Eigler *et al.*, ERK1/2 inhibition promotes robust myotube growth via CaMKII activation resulting in myoblast-to-myotube fusion. *Dev. Cell* **56**, 3349–3363.e6 (2021).
51. G. M. Lu *et al.*, FGF2-induced PI3K/Akt signaling evokes greater proliferation and adipogenic differentiation of human adipose stem cells from breast than from abdomen or thigh. *Aging (Albany, NY)* **12**, 14830–14848 (2020).
52. A. Lebaschi *et al.*, Animal models for rotator cuff repair. *Ann. N. Y. Acad. Sci.* **1383**, 43–57 (2016).
53. A. E. C. Nichols, K. T. Best, A. E. Loiselle, The cellular basis of fibrotic tendon healing: Challenges and opportunities. *Transl. Res.* **209**, 156–168 (2019).
54. T. J. Wess, Collagen fibril form and function. *Adv. Protein Chem.* **70**, 341–374 (2005).
55. X. Tang *et al.*, The treatment of muscle atrophy after rotator cuff tears using electroconductive nanofibrous matrices. *Regen. Eng. Transl. Med.* **7**, 1–9 (2021).
56. N. S. Shemshaki *et al.*, Efficacy of a Novel Electroconductive Matrix To Treat Muscle Atrophy and Fat Accumulation in Chronic Massive Rotator Cuff Tears of the Shoulder. ACS Biomater. Sci. *Eng.* **9**, 5782–5792 (2023).
57. H. H. Yoon *et al.*, Dual roles of graphene oxide in chondrogenic differentiation of adult stem cells: Cell-adhesion substrate and growth factor-delivery carrier. *Adv. Funct. Mater.* **24**, 6455–6464 (2014).
58. S. Pan *et al.*, Graphene oxide–PLGA hybrid nanofibres for the local delivery of IGF-1 and BDNF in spinal cord repair. *Artif. Cells, Nanomed. Biotechnol.* **47**, 651–664 (2019).
59. M. Zhou *et al.*, Graphene oxide: A growth factor delivery carrier to enhance chondrogenic differentiation of human mesenchymal stem cells in 3D hydrogels. *Acta Biomater.* **96**, 271–280 (2019).
60. N. S. Shemshaki *et al.*, Electroconductivity, a regenerative engineering approach to reverse rotator cuff muscle degeneration. Regen. *Biomater.* 10 (2023).